AIAA JOURNAL
Vol. 40, No. 9, September 2002

Probabilistic Approach to Free-Form Airfoil Shape Optimization Under Uncertainty

Luc Huyse*
Southwest Research Institute, San Antonio, Texas 78228-0510
Sharon L. Padula†
NASA Langley Research Center, Hampton, Virginia 23681-2199
R. Michael Lewis‡
College of William and Mary, Williamsburg, Virginia 23187-8795
and
Wu Li§
Old Dominion University, Norfolk, Virginia 23529

Free-form shape optimization of airfoils to minimize drag directly poses unexpected difficulties. Practical experience has indicated that a deterministic optimization for discrete operating conditions can result in dramatically inferior performance when the actual operating conditions are different from the (somewhat arbitrarily selected) design conditions used during the optimization. Extensions from single-point to multipoint optimization have proven unable to remedy this problem of localized optimization adequately near the sampled operating conditions. An intrinsically statistical approach is presented, and how the shortcomings of traditional optimization methods can be overcome is demonstrated. We discuss two algorithms. The first one is based on a numerical evaluation of the expectation integral during each optimization step. The second one is based on a closed-form second-order analytic approximation of the integration. The airfoil geometry optimization example (inviscid Euler flow) also reveals how the relative likelihood of each of the operating conditions is automatically taken into consideration during the optimization process. This is a key advantage over the use of multipoint methods.

Nomenclature

c	=	chord length
c_l	=	lift coefficient
c_l^*	=	target lift coefficient
$c_p d$	=	wave drag coefficient
$\boldsymbol{d}$	=	design vector
$f_X(x)$	=	probability density function of the random variable X
M	=	freestream Mach number
M_{div}	=	divergence Mach number
$\bar{M}$	=	mean freestream Mach number
m	=	number of design conditions considered
t/c	=	relative thickness of airfoil
var( )	=	variance of random variable
w	=	weighting coefficient
x, y	=	Cartesian coordinates of the spline control nodes that describe the airfoil geometry
α	=	angle of attack, deg
ϵ	=	random error
ρ	=	risk associated with design
$\nabla_M c_d$	=	first derivative of c_d with respect to M

Introduction

DURING the design process of a structure or device, appropriate values need to be selected for the design variables, such that the performance of the design is optimized. The specification of one or more design operating conditions allows the engineer to use deterministic optimization schemes. An example hereof is found in airfoil design, where a cruise Mach number and target lift coefficient are specified and the objective is to minimize the drag under those constraints.

Optimization of an analytical model is a tool to develop better designs. Recent advances in computing power and the development of more accurate computational fluid dynamics (CFD) codes should, at least in theory, allow one to compute the optimal shape of an airfoil for a particular application. Unfortunately, the use of deterministic optimization techniques leads to unexpected problems. Broadly speaking, two families of shape optimization strategies can be distinguished:

1) The first strategy is knowledge-based: An empirical algebraic expression of airfoil geometry is selected and the optimization process determines the optimal values for the coefficients (such as maximum thickness, camber, radius of leading edge, etc.) that appear in this expression.

2) The second strategy is free-form: The geometry is represented by a linear combination of general basis functions (such as splines). In principle, using more basis functions to define the geometry leads to a geometry representation with higher resolution.

The major advantage of the first approach is that it typically involves a limited number of design variables and results in conventional airfoil geometries. The free-form approach does not restrict the geometry of the airfoil and has the potential to discover some truly innovative designs. However, the free-form approach can also lead to high-frequency oscillations and/or difficulty in enforcing geometry constraints. See Ref. 1 for a complete discussion of airfoil parameterization options.

Another concern with shape optimization of airfoils is the sensitivity of the final optimal design to small manufacturing errors or fluctuations in the operating conditions. Tightening the tolerances in the manufacturing process may prove prohibitively expensive or practically impossible to achieve. It is expensive to produce such a precise design and impossible to maintain this pristine shape during routine flight operations. Moreover, a certain variability or

Received 12 September 2001; revision received 12 April 2002; accepted for publication 16 April 2002.

*Research Engineer, Reliability and Engineering Mechanics; luc.huyse@swri.org. Member AIAA.
†Senior Research Engineer, Multidisciplinary Optimization Branch; s.l.padula@larc.nasa.gov. Associate Fellow AIAA.
‡Assistant Professor, Department of Mathematics; buckaroo@math.wm.edu. Member AIAA.
§Professor, Department of Mathematics and Statistics; wli@odu.edu.

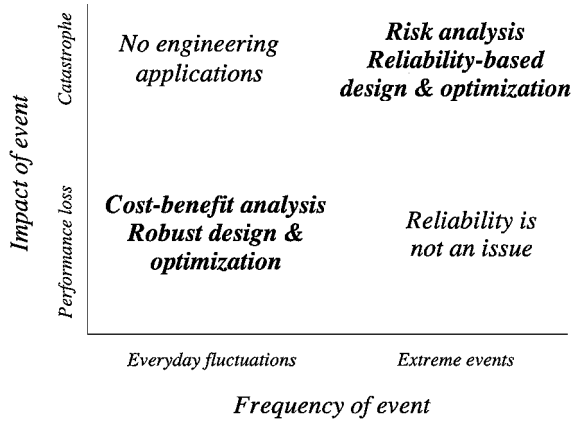

Fig. 1 Uncertainty classification.

uncertainty in the operating conditions, for example, cruise Mach number, cannot be avoided. The sensitivity of the design performance to such relatively small uncertainties provides an incentive to use so-called robust optimization methods, which directly include the effects of the uncertainties on the performance of an optimized design.

Several different nondeterministic approaches (Taguchi methods, bounds-based, minimax, fuzzy, and probabilistic methods) can be used to achieve robustness of an optimal design. This research deals with robust design of airfoils to address uncertain operating conditions. Other researchers have worked in the field of reliability-based design and have studied reliability-based optimization of aerospace structures and compressor blades (for example, Refs. 2 and 3). Figure 1 explains the difference between robust and reliability-based design problems. In an engineering context, risk is typically defined as the product of the probability and the impact or consequence of an event.[4] Structural reliability techniques are particularly useful to assess the risk associated with infrequent but potentially catastrophic events (such as turbine blade failures[5]). On the other hand, robust optimization techniques account for the impact of everyday fluctuations of parameters (such as variations in cruise Mach number) on the overall design performance, assuming that no catastrophic failures occur.

Achieving Robustness

Developing optimization methods that result in more robust designs sounds appealing. The term robustness means a variety of things; there are four popular goals of robust design:

1) Identify designs that minimize the variability of a manufactured product under uncertain processing conditions. This is the objective of Taguchi methods[6]; they are most practical when the variance of the objective can be reduced at negligible cost.

2) Mitigate the detrimental effects of the worst-case performance. This is the objective of minimax strategies.[7] They choose a design with the best worst-case performance.

3) Obtain a uniform improvement of the performance function over the entire range of the operating conditions.[8]

4) Provide the best overall performance over the entire lifetime of the structure or device.[9]

In this paper, the focus is on the last definition: robust optimization that tries to achieve the best expected performance (or minimal expected cost) with respect to uncertain operating conditions. We introduce a nondeterministic method and compare its results with the more traditional multipoint optimization method.

To our knowledge, nondeterministic approaches are quite new to aerodynamic optimization. First, we define a practical airfoil shape optimization problem that will be used to compare various optimization strategies. Then, an overview of existing deterministic attempts at introducing robustness is presented. Subsequently, we discuss an inherently statistical approach based on Von Neumann–Morgenstern's maximum expected value criterion (see Ref. 9). Numerical results for a two-dimensional airfoil shape optimization problem obtained using different optimization strategies are compared.

Airfoil Optimization Problem in Transonic Regime

Problem Formulation

In this section we present a transonic airfoil optimization problem to which the various direct optimization strategies will be applied. All optimizations use the NACA-0012 airfoil with a sharp trailing edge as the baseline geometry. The NACA-0012 is represented by splines using 23 control nodes. Because the NACA-0012 is not suitable for the transonic regime, substantial improvements are to be expected.

The design variables in the optimization problem are given by the vertical positions of the control nodes and the angle of attack α. Three control nodes are in locked positions: one at the leading edge and a double control node at the trailing edge. Box constraints limit the maximum movement of each of the 20 spline control nodes (Fig. 2). This results in a reduced thickness t/c of the optimized airfoils; typically, the final t/c ratio is about 0.1, which means that the reduction of the wave drag is at least in part due to the reduction of the relative thickness t/c.

The inviscid Euler equations for the flow are discretized on unstructured meshes.[10] The sensitivities of both lift and wave drag with respect to the design parameters are efficiently calculated using a discrete adjoint formulation.[11]

The objective is lift-constrained wave drag minimization over the Mach range $M \in [0.7, 0.8]$:

$$\min_{d \in D} \quad c_d(\boldsymbol{d}, M)$$
$$\text{subject to} \quad c_l(\boldsymbol{d}, M) \geq c_l^* \qquad \text{over } M \in [0.7, 0.8] \qquad (1)$$

where $\boldsymbol{d}$ is the vector of design variables and $\boldsymbol{D}$ is the design space. The minimum lift constraint corresponds to typical values found for commercial transport airliners.[12] In this study, the Mach number is the only uncertain parameter; no additional model uncertainties are included. No constraints are imposed on the pitching moment.

Grid Convergence

Four different grid resolutions were used to check the convergence of the flow solution, especially the wave drag c_d. The far-field boundary for grid 1 is located at 10 chord lengths. For grids 2, 3, and 4 (Fig. 3), the far-field boundary is located at 50 chord lengths. For each of the grids the number of elements along both the airfoil inner boundary and the circular far-field boundary are

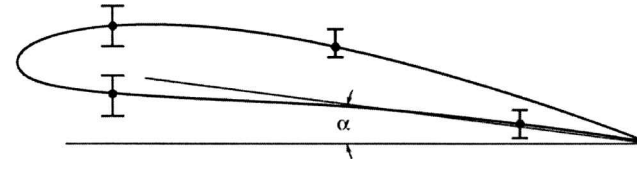

Fig. 2 Design variables and box constraints for the airfoil (schematic).

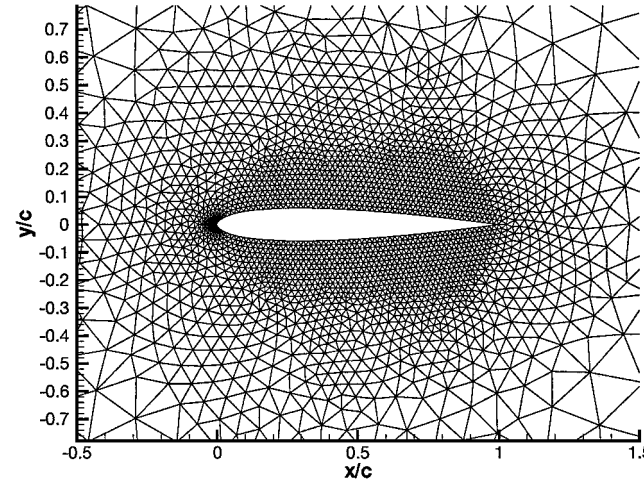

Fig. 3 Baseline NACA-0012 airfoil: grid 2.

specified in Table 1. Grid generator details are available in Ref. 13. Figure 4 shows the drag profile in the Mach range $M \in [0.7, 0.8]$ for a constant angle of attack $\alpha = 1.5$ deg. Grids 1 and 2 are considered low-fidelity models, whereas grid 4 is the high-fidelity or truth model. Because grid 1 is too coarse, we used grid 2 for the actual optimizations. On completion of the optimization, a check using grids 3 or 4 can be performed. The idea is to use the fast low-fidelity grids as much as possible, but to verify the results using the high-fidelity grids.[14]

Figure 4 reveals that grids 1 and 2 overestimate the wave drag. The overestimation of grid 1 has a double cause: It is an extremely coarse grid, and the far-field boundary is located at 10 chord lengths only. The overestimation in grid 2 is smaller than for grid 1 and occurs in equal amounts irrespective of the Mach number. There is virtually no difference in the drag profiles computed on grids 3 and 4. Very similar grid-induced differences in the drag profiles were observed in the Mach sweep curves (c_d as a function of M) for the optimized airfoils.

Table 1 Grids used in examples: grid 1 is generated using Double9; all other grids are generated using AFLR[13]

Grid	Airfoil element	Far-field element	Nodes	Faces	Elements
1	129	32	411	1,170	822
2	124	32	3,060	9,025	6,120
3	250	64	9,246	27,424	18,492
4	500	128	32,067	95,574	64,134

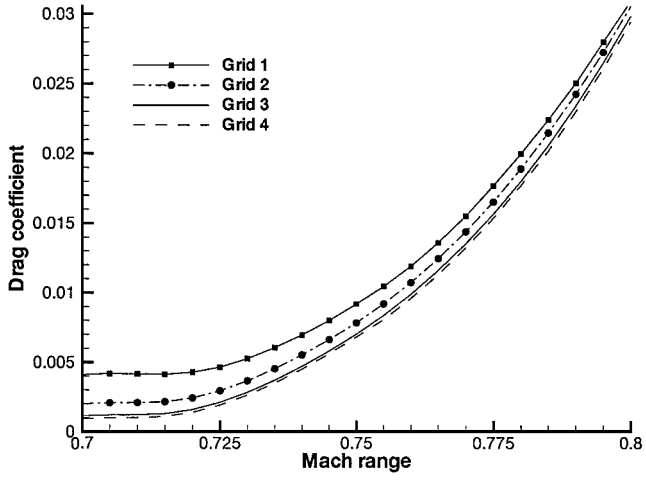

Fig. 4 Drag profiles for NACA-0012 on all four grids (α = 1.5 deg).

Deterministic Approach to Airfoil Shape Optimization

Single-Point Optimization

In a deterministic context, aerodynamic shape optimization of airfoils is concerned with obtaining the most aerodynamically favorable geometry for fixed, either known or assumed, operating or design conditions. Consider the practical case where the drag c_d is to be minimized at a given, fixed freestream Mach number M_1:

$$\min_{d \in D} \quad c_d(\boldsymbol{d}, M_1)$$
$$\text{subject to} \quad c_l(\boldsymbol{d}, M_1) \geq c_l^* \tag{2}$$

This deterministic, single-point optimization model is not necessarily an accurate reflection of the reality. The formulation in Eq. (2) contains no information regarding off-design condition performance. It is documented by other researchers[15] that, with formulation Eq. (2), the drag reduction is attained only over a narrow range of Mach numbers (Fig. 5a). In this paper we will refer to this as localized optimization.

It can be concluded that the real problem is not with the optimization code, which is likely to perform well, but with the problem formulation of Eq. (2). The local optimization effect is particularly worrisome if substantial variability is associated with the operating conditions. Explicit tradeoffs between different design conditions should be considered in the problem formulation.

Multipoint Optimization

A straightforward, but heuristic, approach to avoid localized optimization is to consider different Mach numbers and to generalize the objective in Eq. (2) to a linear combination of flight conditions (m in total):

$$\min_{d \in D} \quad \sum_{i}^{m} w_i c_d(\boldsymbol{d}, M_i)$$
$$\text{subject to} \quad c_l(\boldsymbol{d}, M_j) \geq c_l^* \qquad \text{for} \qquad j = 1, \ldots, m \tag{3}$$

Practical problems arise with the selection of the flight conditions M_i and with the specification of the weights w_i. There are no clear theoretical principles to guide the selection, which is, in fact, largely left up to the designer's discretion (see, for example, Refs. 15–17).

With the multipoint formulation of Eq. (3), an improved c_d can be realized over a wider range of Mach numbers M (Ref. 15). However, this formulation is still unable to avoid localized optimization. In fact, multiple bumps might appear on the airfoil, one associated with each flight condition M_i. In the transonic regime, each bump occurs at the shock foot location for each of the sampled Mach numbers.[15]

An illustration of localized optimization is given in Fig. 6. This optimization was performed on grid 2, with target lift $c_l^* = 0.4$, using equal weight ($w_i = 0.25$) for each of four design conditions. Because the drag is highest at the higher Mach numbers, the drag at those Mach numbers has been reduced significantly during the

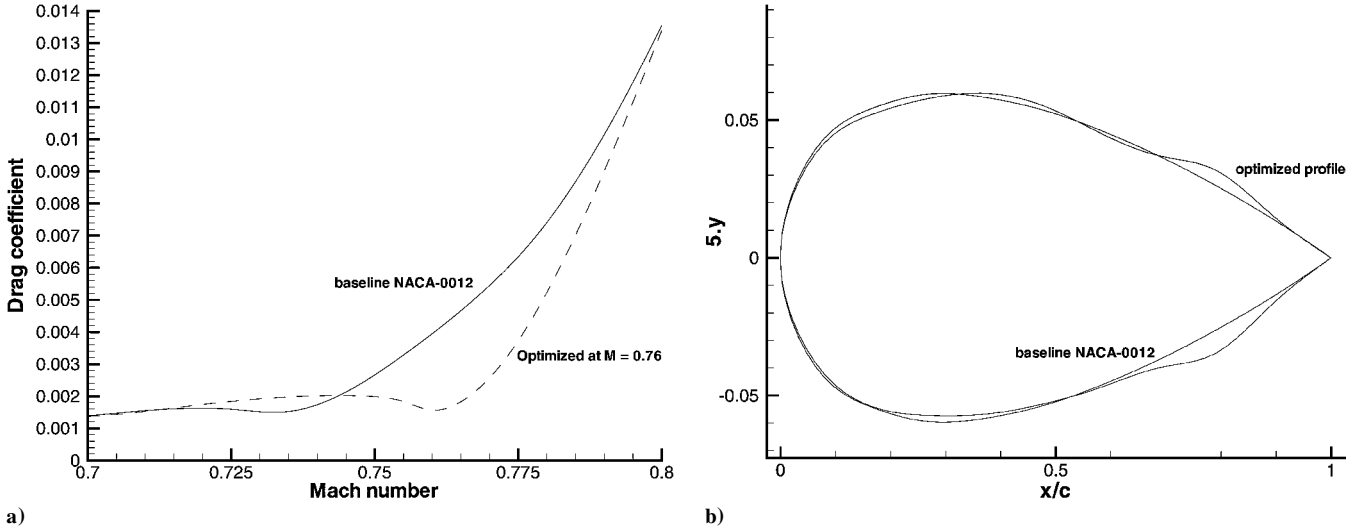

Fig. 5 Single-point optimization using grid 2 and $c_l^* = 0.2$: drag profile and airfoil geometry.

optimization process. Figure 6 clearly indicates that these drag improvements occur only at particular Mach numbers and are rapidly lost when the actual Mach number deviates from the selected design Mach numbers. This effect is particularly pronounced for the high Mach numbers.

Figure 7 explains this in more detail using two contour plots of the local Mach number. The operating conditions (freestream Mach numbers) are very similar, but the flow solutions (local Mach number) are very different. The multipoint optimization process introduces geometric features to the airfoil that lock the shock waves in place. Because we used four point optimization, we have four shocks (see also Ref. 15). In Fig. 7a, four shocks can be distinguished along the top surface. In Fig. 7b, the most-aft shock has basically disappeared. The optimizer has locally modified the geometry and eliminated the shock associated with Mach 0.8, which was one of the design conditions.

Alternative Strategies

Because derivatives have to be calculated for each variable at various operating conditions, the computational cost associated with multipoint optimization using CFD is substantial. Alternate methods, which incorporate some common-sense engineering knowledge into the optimization process, may be a valuable and cheaper alternative. One such example is the method of the weighted average of geometries (WAG).[16]

In the WAG method, the optimal design is obtained as a weighted average of n single-point optimal designs, each one of them corresponding to one of the n chosen operating conditions. The weighting factors depend on the relative importance of each operating condition [similar to the w_i in Eq. (3) for multipoint design]. However, a key feature of this optimization method is that it still requires the formulation of some aggregate objective function, which describes the overall, or aggregate, performance of the design as a function of the variable Mach number.

The method requires the designer to select appropriate weights before the optimization process is started. As a result, the quality of the optimum solution is directly related to the actual choice of the selected weights. Sometimes such a choice may be quite difficult to make, and this selection introduces some arbitrariness in the design process.

In the analytic hierarchy process,[18] the weights can be changed during the optimization process itself. For each optimization step, a pairwise comparison matrix can be defined that indicates the relative importance of each of the design conditions at the current iteration step in the optimization process. The method monitors the optimization progress and gives the designer the opportunity to adjust the relative weight accordingly.

The need to adjust the weights is eliminated altogether in Messac's physical programming method.[19] In this method, the designer expresses preferences concisely using a classification function. Examples thereof are smaller-is-better, range-is-better, and must-be-larger. In addition a degree of desirability is associated with each of these classes, ranging from unacceptable to highly desirable. By the use of these preference functions, the different design metrics are all mapped onto a dimensionless scale on which the actual optimization is performed. The method seems quite well suited for problems where various objectives have different dimensions, such as range and speed.

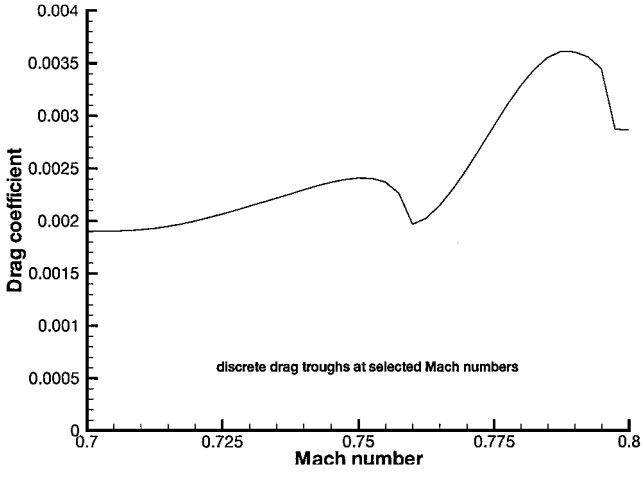

Fig. 6 Drag profile for a four-point optimization using grid 2 and $c_l^* = 0.4$; operating conditions are $M = 0.7, 0.733, 0.766$, and 0.8.

Nondeterministic Approaches

Design as a Decision-Making Process

During the airfoil design process, appropriate values of the design variables $\boldsymbol{d}$ need to be selected that optimize the performance or the utility of the airfoil design. The designer has full control over the design variables, such as the geometry of the structure and the type and grade of materials used for it, but the operating conditions of a structure or device, such as the loads or the operating speeds, will typically vary during the design lifetime.

Because each operating condition parameter may take on a range of values over the lifetime of the design, it is possible to collect their histograms (and joint histograms). From a subjectivist point of view, the parameters representing operating conditions are then effectively modeled as random variables.

The preceding section indicated that a specific airfoil design may perform exceptionally well for a selected freestream Mach number M_1, but may perform poorly for other values of M. The impact of the uncertainty of M on the design performance should be taken into account when the quality of a particular design is assessed.

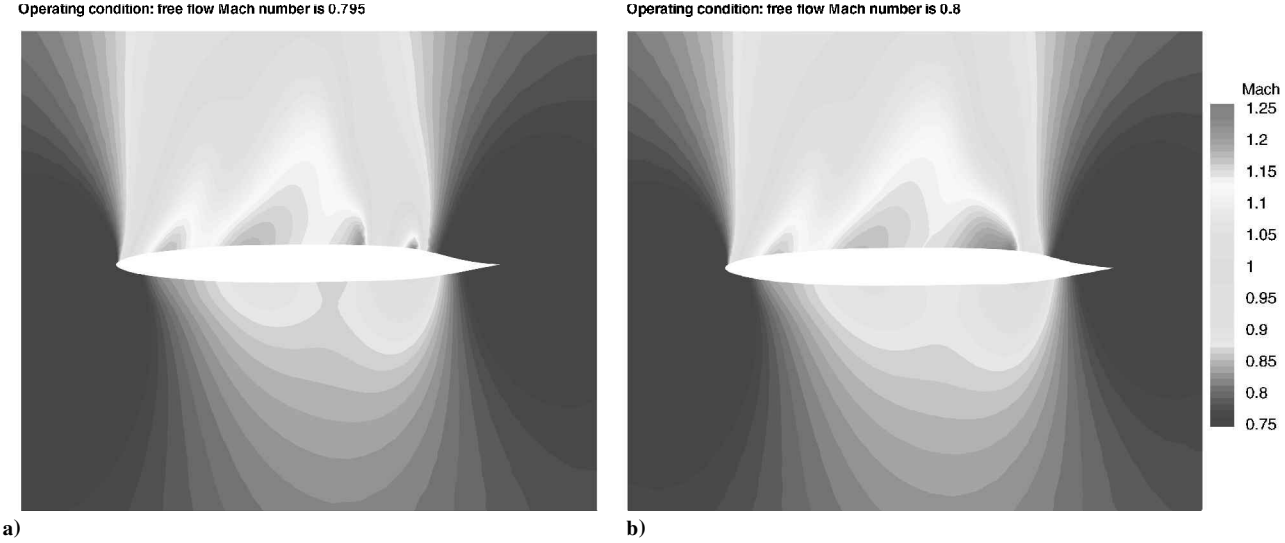

Fig. 7 Local Mach number for two free-flow conditions after four-point optimization using grid 2 and $c_l^* = 0.4$.

Bounds-Based Methods

Bounds-based methods recognize that a designer does not have access to data with unlimited precision: some of these data are intrinsically variable (operating conditions), some of them can be collected or measured with limited precision only (sampling error), and sometimes the measurement process itself is imperfect, which introduces bias. Gu et al.[20] recognize that analytical and numerical models fail to yield the correct result; they call the difference between the average experimental data and the value obtained from the analysis code the bias error. All other errors are lumped into random variability. They assign bounds to each of those uncertainties and develop a methodology to incorporate the bounds directly into the multidisciplinary design optimization.[21]

In our opinion, the main drawback of bounds-based methods is that they essentially assume that all outcomes within the specified bounds are equally likely to occur. This conflicts with the intuitive sense that, by their very definition, extremes should occur with much lower frequency than average or normal behavior. This implies that error bounds will grow quite rapidly as more and more uncertainties are explicitly considered in the design or optimization process. An explicitly statistical approach takes the relative likelihood of combined extremes vs other joint occurrences into account by means of the probability density function (PDF). In summary, the bounds-based approach has two drawbacks:

1) Bounds cannot always be identified accurately.

2) Bounds-based methods are overconservative.

Explicitly Statistical Problem Formulation

Reconsider the basic problem in Eq. (1): Minimize the drag c_d over a range of free-flow Mach numbers M while maintaining the lift $c_l \geq c_l^*$. Note that M is now treated as a random variable. The optimization problem Eq. (2) is now interpreted as a statistical decision-making problem.

In the presence of uncertainty, a designer is forced, in effect, to take a gamble. Under such circumstances, rather than naively hoping for the best or conservatively focusing on the worst, the right decision consists of the best possible choice of the design, whether favorable or unfavorable operating conditions occur. All decision problems have two essential characteristics[9]:

1) A choice, or sequence of choices, must be made among various possible designs.

2) Each of these choices corresponds to a performance, but the designer cannot be sure a priori what this performance will be. The exact performance also depends in part on unpredictable events, in this case the operating conditions.

In our example, only one initial choice regarding the design needs to be made; the airfoil geometry must be selected. According to the Von Neumann–Morgenstern statistical decision theory (see Ref. 9), the best course of action in the presence of uncertainty is to select the design airfoil that leads to the lowest expected drag. This is commonly known as the maximum (or minimum) expected value criterion. The risk ρ, associated with a particular design $\boldsymbol{d}$, is identified as the expected value of the perceived loss associated with the design. The best design or decision, which minimizes the overall risk, is referred to as Bayes's decision. In our problem formulation, Bayes's risk ρ^* and Bayes's decision $\boldsymbol{d}^*$ are given by Eqs. (4) and (5), respectively:

$$\begin{aligned} \rho^* = \min_{d \in D} \quad & \int c_d(\boldsymbol{d}, M) f_M(M)\, \mathrm{d}M \\ \text{subject to} \quad & c_l(\boldsymbol{d}, M) \geq c_l^* \qquad \text{for all} \qquad M \end{aligned} \tag{4}$$

or

$$\rho^* = \int c_d(\boldsymbol{d}^*, M) f_M(M)\, \mathrm{d}M \tag{5}$$

where $f_M(M)$ is the PDF of the free-flow Mach number M.

The practical problem with formulation (4) is that integration is required in each of the optimization steps. Because the objective function c_d is computationally expensive to evaluate, this approach, although theoretically sound, becomes prohibitively expensive. Therefore, a computational scheme that minimizes the number of function calls is desirable.

In addition, the physical and mathematical models themselves used for the objective function will not be error free. Each of these model errors can be treated as a random variable. Their effect on the optimal solution is readily assessed by extending the integration over these additional random variables.

Note that in this problem we are not concerned with rapid Mach number variations. Only slowly varying Mach numbers (steady states) are considered. Because the Mach number is constant for a certain length of time, the angle of attack can be adjusted to reach the required lift c_l^*. Consequently, the lift constraint in Eq. (4) is not probabilistic but remains deterministic.

Analytic Approximation of the Expectation Integral

When the variability of the free-flow Mach number M is not too large, a second-order Taylor series expansion of c_d around the mean value $\bar{M}$ may be a sufficiently accurate model of the variation of the drag c_d with respect to M:

$$c_d(\boldsymbol{d}, M) = c_d(\boldsymbol{d}, \bar{M}) + \nabla_M c_d \cdot (M - \bar{M}) + \tfrac{1}{2} \nabla_M^2 c_d \cdot (M - \bar{M})^2 \tag{6}$$

When substituted in Bayes's risk expression (4), the linear term $\nabla_M c_d \cdot (M - \bar{M})$ in Eq. (6) disappears after integration over M because the Taylor series is built around the mean value $\bar{M}$. Bayes's risk Eq. (5) can be approximated by

$$\begin{aligned} \rho^* = \min_{d \in D} \quad & [c_d(\boldsymbol{d}, \bar{M}) + \mathrm{var}(M) \nabla_M^2 c_d(\boldsymbol{d}, \bar{M})] \\ \text{subject to} \quad & c_l(\boldsymbol{d}, M) \geq c_l^* \qquad \text{for all} \qquad M \end{aligned} \tag{7}$$

where $\mathrm{var}(M)$ denotes the variance of the Mach number M.

It seems that we have substituted an integration with an almost equally expensive computation of a second-order derivative. However, this theoretical result provides additional insight into the problem. It follows from Eq. (7) that the variability of M can affect the optimal design only if the objective function c_d is highly nonlinear in this parameter. This is the case near the drag divergence Mach number M_{div}, where the drag undergoes a sharp increase (see Fig. 5a).

In mathematical terms, the advantage of working with expected utilities is that the minimum is second-order accurate with respect to variations in the parameters. This ensures a more global solution and localized optimization will be avoided. This can also be explained in an intuitive manner: The second-order derivative is a measure for the curvature. Because this curvature is now a part of the objective function, a design that results in a drag trough or cusp at $\bar{M}$ as found in the optimal solution in Fig. 5 will not be accepted by the optimizer. The high curvature of the cusp at $\bar{M}$ would increase the objective in Eq. (7), and excessive localized optimization will be avoided.

Direct Numerical Evaluation of Expectation and Comparison with Multipoint Optimization

The integration with respect to M in Eq. (4) can also be performed numerically. Irrespective of the chosen integration scheme, integral (4) can formally be written as (m integration points)

$$\rho^* = \min_{d \in D} \left[\sum_{k=1}^{m} w_k \cdot c_d(\boldsymbol{d}, M_k) + \epsilon(m) \right] \tag{8}$$

where the integration error $\epsilon(m) \to 0$ as $m \to \infty$.

Formulation Eq. (8) is strikingly similar to Eq. (3). It is, therefore, interesting to analyze how Bayes's decision $\boldsymbol{d}^*$ compares with the multipoint solution and exactly how localized optimization is avoided. In the multipoint approach, the design condition Mach numbers and weights need to be selected by the designer. In the statistical approach, the Mach numbers are determined by the integration scheme. The weights are directly related to the relative importance of each Mach number through the integration over the probability density. In short, the statistical approach removes the arbitrariness from the weighting process. Comparison of Eq. (3) with

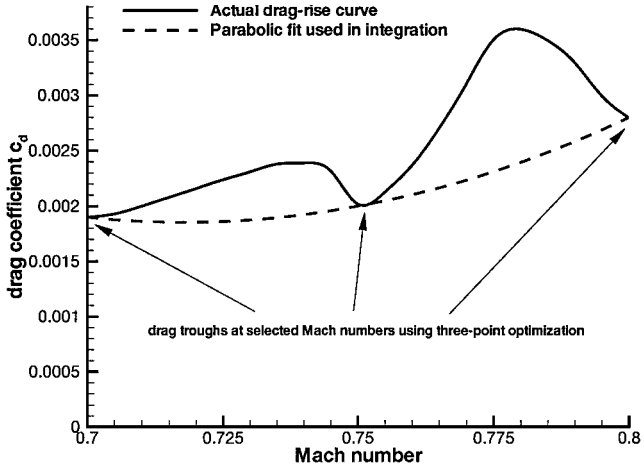

Fig. 8 Final drag rise obtained for three-point optimization; actual drag rise is no longer approximated well by a parabola.

Eq. (8) reveals the shortcoming in the multipoint formulation that causes localized optimization. Numerical integration of Eq. (4) results in Eq. (8) and includes a random, zero-mean error term $\epsilon(m)$, which decreases as the number of sampling points increases. The multipoint optimization Eq. (3) differs from Eq. (8) only in the sense that this error term is not explicitly considered in the objective function. However, omitting this term alters the structure of the problem at hand.

The multipoint optimization looks for the design, which minimizes the weighted sum of the goal function c_d, evaluated in the m specified points M_k. There is no control over the objective function c_d in the neighborhood around these m sampling points. Experience by other researchers[22] and the preceding deterministic examples have indicated that significant troughs in plots of c_d vs M are introduced near the sampling points, as illustrated in Fig. 8. In effect, multipoint optimization will prefer a design $\boldsymbol{d}_1$ over a design $\boldsymbol{d}_2$ even when design $\boldsymbol{d}_1$ is considerably worse than design $\boldsymbol{d}_2$ in all but the m specified sampling points. The multipoint formulation allows the optimizer to mold the goal function c_d to its own advantage. What was originally a random integration error is no longer random, and the discrete sum in Eq. (3) no longer approximates the integral in Eq. (4) at all.

This undesirable behavior is avoided if we can prevent the optimizer from exploiting the approximation error in Eq. (8) to its own advantage. We need to make sure that the discrete sum in Eq. (8) remains a good approximation of the integral in Eq. (4) throughout the optimization process (Fig. 8). An elegant solution is to add a small random perturbation to the sampling points M_k in the evaluation of the integral. This ensures that the optimizer maximizes the performance not just for m specific values of M_k, but for any set of values $M_k, k = 1, \ldots, m$. To minimize the loss of accuracy in the integration due to random location of the integration points, stratified sampling can be used to generate the values of M_k. Our experience with the spline-based integration also suggests that the sampling points should not be allowed to be arbitrarily close to each other.

However, with this scheme, a repeated evaluation of the objective function c_d for identical values of the design parameters $\boldsymbol{d}$ will lead to different results. This makes it hard to identify whether a new design is really better than a preceding one, or if the improvement should be attributed to random fluctuations instead. When a trial solution $\boldsymbol{d}$ is still far away from the optimal solution $\boldsymbol{d}^*$, large improvements Δc_d can be expected. This means that a very crude integration, which requires very few function evaluations, will suffice in the early stages of the optimization. The improvement of the goal function is expected to be smaller closer to the optimal solution, and more sampling points M_k will be required to keep the integration error small enough. Current research focuses on the development of a strategy that takes maximum advantage of this effect.

Application to a Two-Dimensional Airfoil in Transonic Regime

Various Optimization Strategies

In this section we compare results for the various optimization strategies presented in this paper. We apply the sequential linear programming[23] (in iSIGHT Ver. 5.5, a product of Engineous Software, Inc.[24]) to the lift-constrained airfoil optimization problems introduced earlier. We assume that the Mach number variations are bounded between 0.7 and 0.8. In particular, the following optimization formulations are compared:

1) In single-point optimization, various Mach numbers are considered as the design point.

2) In, multipoint optimization, each of the m design conditions has predetermined fixed weights [see Eq. (3)].

3) In expected value optimization, to allow for a direct comparison with the multipoint results, $f_M(M)$ in Eq. (4) is a uniform distribution.

4) The approximate second-order second-moment (SOSM) method is based on a mean value $\bar{M} = 0.75$; the variance is set equal to the variance of the uniform PDF used in formulation 3 [see Eq. (7)].

Note that formulations 2 and 3 require comparable omputational effort.

Single-Point Optimization Results

The single-point case has 21 design variables: the angle of attack α and the vertical positions of the 10 spline control nodes at both the top and bottom surface of the airfoil. Figure 5a indicates that a dramatic reduction of the drag c_d is obtained at $M = 0.76$ (also see the first entry in Table 2), but it also reveals that this gain is rapidly lost when the free-flow Mach number is away from this design value.

The geometry plot in Fig. 5b illustrates what happens. During the optimization a distinct bump is formed on the airfoil surface. The optimizer takes advantage of all degrees of freedom to achieve the lowest possible drag at the design Mach number $M = 0.76$, irrespective of what happens to the drag at other Mach numbers. Obviously, there is a penalty to be paid for this: Even though the drag reduction at the design Mach number is 60%, the total average reduction over the entire Mach range is only 18%. The use of a single-point optimization would lead to the false conclusion that a 60% improvement has been achieved; the actual realized gain is only 18%. Of course, because only loose box constraints were applied to the control nodes, some of this drag reduction must be attributed to a reduction of the relative thickness t/c. The t/c ratio for all optimized airfoils is about 0.1.

Qualitatively similar results are obtained for other lift values and design Mach numbers and are summarized in Table 2. The localized optimization, illustrated in Fig. 5, was previously documented by Drela.[15] Figure 9 shows that the bump on the airfoil moves aft when the Mach number increases. This pushes the shock toward the trailing edge and postpones the drag rise. Figure 10 indicates that the choice of the design Mach number considered in the optimization has an enormous impact on the final drag profile and airfoil geometry. Figure 10 shows that simply selecting the mean Mach number ($M = 0.75$) or the Mach number with highest drag ($M = 0.80$) does not guarantee good overall performance over the entire Mach range.

Table 2 Comparison of the drag reductions with respect to the original NACA-0012 at the design point and over the entire Mach range for single-point optimization results

Target lift c_l	Design Mach number M	Δc_d at the design point, %	Total reduction Δc_d over Mach range, %[a]
0.2	0.76	60	18
0.4	0.75	84	52
0.6	0.72	85	30
0.6	0.75	87	53
0.6	0.78	91	78
0.6	0.80	75	57

[a]This is the relative reduction of the area under the curve c_d vs M compared to the baseline NACA-0012.

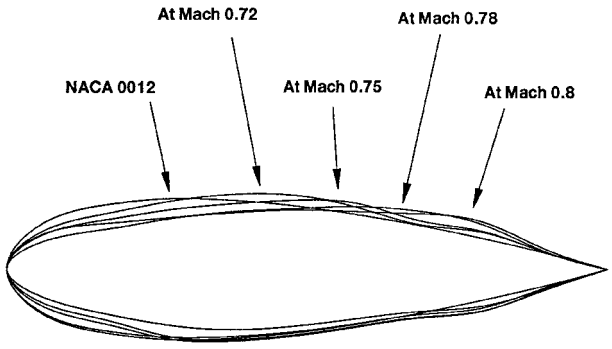

Fig. 9 Bump locations for different design Mach numbers for single-point optimization ($c_l^* = 0.6$).

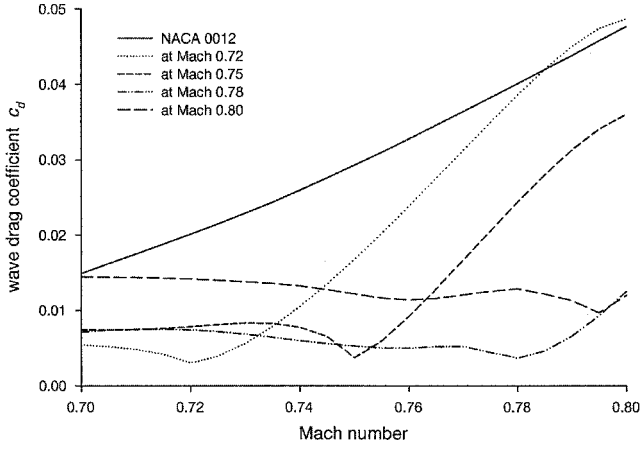

Fig. 10 Single-point optimization results for various design Mach numbers ($c_l^* = 0.6$).

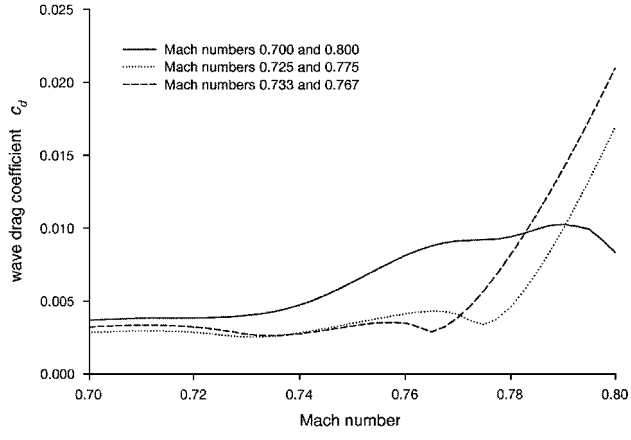

Fig. 11 Optimal drag profiles obtained using different two-point optimization strategies ($w_1 = w_2 = 0.5$ and $c_l^* = 0.6$).

Multipoint Optimizations

The constrained multipoint optimization has $(20 + m)$ design variables: the same 20 y coordinates that describe the geometry and m angles of attack. Because of compressibility effects, the minimum angle of attack for which the lift constraint is satisfied decreases with increasing free-flow Mach number.[25] Consequently, each design condition adds one additional angle-of-attack design variable.

The two-point optimization results shown in Fig. 11 illustrate the shortcomings of this method, which were also reported by Drela.[15] Optimization at selected Mach numbers results in clearly distinguishable drag troughs at each of the design Mach numbers (Figs. 6 and 7). Drela leaves it up to the designer to determine which Mach numbers to include in the objective in Eq. (3) and which weights to choose. Three reasonable selections are compared with each other

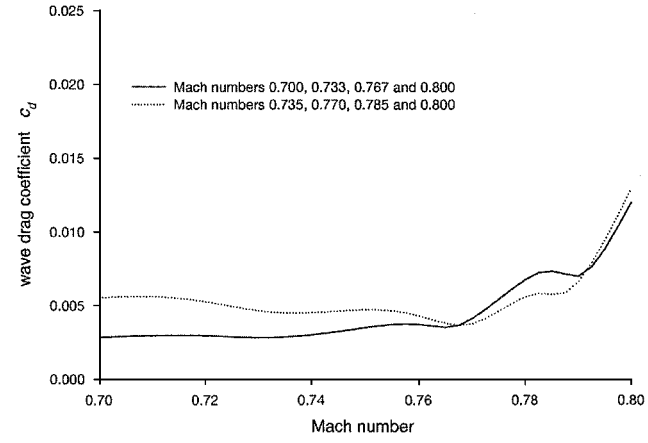

Fig. 12 Drag profile obtained using different four-point optimization strategies ($c_l^* = 0.6$).

in Fig. 11: the endpoints of the Mach interval and selected interior points. It is clear that, at least in this case, the selection of the design conditions has an important effect on the final results. In particular, the selection of the endpoints of the Mach range can lead to troubling results. We observed this in both two-point (Fig. 11) and four-point (Fig. 12) optimization.

Because the drag is higher in the upper part of the Mach range, one may want to include more design Mach numbers from the upper part than from the lower part in the multipoint objective function in Eq. (3). This procedure does not require any additional function calls, keeping the computational cost under control, and it should result in lower drag at the upper end of the Mach range. Figure 12 shows the result of such a multipoint optimization. The selected Mach numbers are indicated on the chart, and the weights w_i are obtained from the numerical integration using four fixed integration points. The maximum drag is reduced, but a penalty is paid near the lower end of the Mach range. In fact, the expected value of the drag has increased from 0.0044 to 0.0055 (assuming a uniform distribution for the Mach numbers between 0.7 and 0.8) compared with the result for evenly spaced Mach numbers. Also, the drag trough at each sample Mach number persists, which indicates localized optimization, as explained earlier.

These results indicate that a multipoint optimization achieves a better overall drag reduction than single-point optimization for both sets of design Mach numbers. This is in line with the findings of other researchers.[15] However, a drag trough may form at or near each of the discrete design points, in which case the drag increases rapidly away from the design points. This effect becomes more pronounced near the high end of the Mach range.

In his study, Drela[15] applies larger weights to the upper part of the Mach range to ensure "that the upper part is not compromised excessively by the less important lower part." Our statistical decision approach suggests that this can only be justified when the higher Mach numbers are more likely to occur, that is, when the PDF $f_M(M)$ is concentrated in the upper Mach range. The weights follow automatically from the integration procedure and are, as such, not directly linked to the actual values of the drag $c_d(M)$.

Expected Value Optimization

For the expected value (EV) scheme the integration points in Eq. (4) are altered slightly for each optimization iteration. Consequently, we can say that the four-point optimization minimizes a weighted sum of four fixed design conditions, whereas the scheme minimizes the weighted sum of any four design conditions. This avoids localized optimization. In this study, relatively small random perturbations are used to change the integration points, but other, more adaptive strategies are currently being researched. The number of integration points must be sufficiently high so that the integration error caused by the change of integration points between optimization steps is smaller than the decrease of drag in that particular optimization step (see subsection Direct Numerical Evaluation of Expectation and Comparison with Multipoint Optimization).

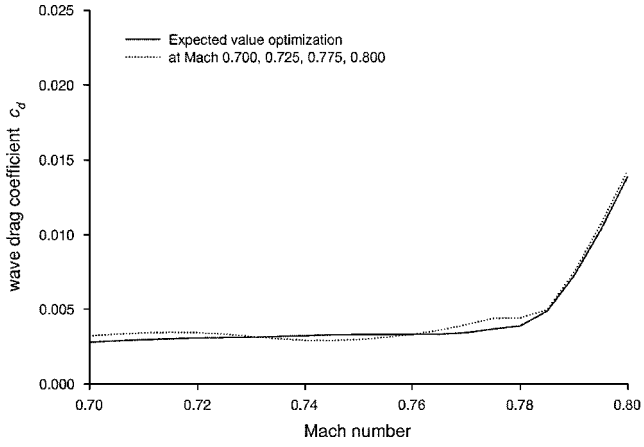

Fig. 13 Drag profile obtained using different optimization strategies ($c_l^* = 0.6$).

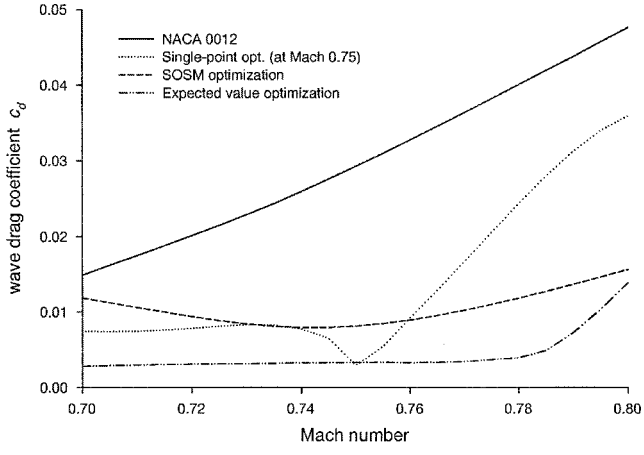

Fig. 14 Comparison of SOSM result with single-point optimization ($c_l^* = 0.6$).

Figure 13 shows that EV optimization strategy results in a much smoother drag profile over the entire Mach range. The integration of drag over the Mach range is performed using spline-based inter/extrapolation. The resulting airfoil geometry is somewhat smoother as well. It may be concluded that, for the same computational effort as multipoint algorithm, the EV scheme results in a superior design.

Obviously, the Mach number will not be uniformly distributed over a given range during operation of an aircraft. A key advantage of the explicitly statistical approach is that the relative importance of each operating condition is automatically accounted for through the PDF. Fluctuations of the Mach number during the flight can be modeled using a truncated Gaussian distribution. Detailed results of this case are presented in Ref. 26.

Approximate SOSM

In this section we present results using the deterministically equivalent problem formulation (7). Equation (7) indicates that first-order sensitivities of the drag c_d with respect to the uncertain variable M do not affect the expected value of the design. The second-order information represents the curvature of the $c_d(M)$ curve, and a large value of curvature near a design Mach number is indicative of localized optimization. In the SOSM formulation, the weighting between the drag and the curvature is determined by the variance of the Mach number. Figure 14 shows a considerable reduction in curvature of c_d vs M using SOSM; for this analysis the variance was set equal to the variance of a uniform distribution between 0.7 and 0.8.

The overall drag reduction is not as good as obtained using explicit numerical integration (Fig. 13), but the computational effort is a lot smaller. The method is particularly useful if higher-order derivatives are available (and numerically reliable) and several uncertain variables are present in the problem. Table 3 compares the relative computational cost for each optimization step. SOSM scales linearly with the number of random variables (one additional second derivative is required for each additional random variable in the optimization), whereas full numerical integration rapidly becomes expensive. Because the method is based on a second-order Taylor-series approximation of the objective function, SOSM will give the best results if the variance of the random variables is relatively small.

Table 3 Number of function/derivative evaluations required per optimization step

Optimization method	1 random variable	3 random variables
Single point	1	1
SOSM[a]	3	7
Expected value (using four-point integration)	4	64

[a]SOSM requires less if analytic derivatives are available.

Summary

The robustness of an optimal solution can be achieved by incorporating the variability of the operating conditions directly into the optimization problem formulation. The practical application shows that a statistical approach leads to smoother airfoil geometries and wave drag profiles than traditional multipoint approaches.

The key feature of the suggested nondeterministic approach is that a designer no longer needs to select which design conditions will be included in the aggregate objective and what their respective weights should be. The new formulation avoids such arbitrary selection of design conditions and weighting factors because they automatically follow from the procedure. The suggested expected value optimization method is computationally similar to existing multipoint optimization, which is widely accepted in industry. This increases the likelihood of acceptance by both designers and theorists alike.

An SOSM approximate integration provides additional insight into the problem. SOSM scales linearly with the number of design variables and may be the only feasible alternative when a large number of uncertainty parameters are involved. This will be the focus of future research.

It can be concluded that airfoil shape optimization on the basis of the Euler equations leads to some interesting candidate designs. However, viscous effects need to be included to achieve more realistic pressure distributions and improved drag predictions.

Acknowledgments

This research was supported by NASA under Contract NAS1-97046 while the first, third, and fourth authors were in residence at the Institute for Computer Applications in Science and Engineering, NASA Langley Research Center, Hampton, Virginia. The authors are indebted to William A. Crossley of the Purdue University School of Aeronautics and Astronautics for his guidance in selecting demonstration problems and to Eric J. Nielsen of the NASA Langley Research Center's Computational Modeling and Simulations Branch for his help with both the FUN2D code and the various grid generators. The very helpful and constructive comments of the anonymous reviewers are appreciated as well.

References

[1]Reuther, J., and Jameson, A., "A Comparison of Design Variables for Control Theory Based Airfoil Optimization," NASA CR-199151, Research Inst. for Advanced Computer Science, Moffett Field, CA, July 1995.

[2]Chiao, M., and Chamis, C., "Optimization of Adaptive Intraply Hybrid Fiber Composites with Reliability Considerations," NASA TM-106632, 1994.

[3]Garzon, V., and Darmofal, D., "Using Computational Fluid Dynamics in Probabilistic Engineering Design," AIAA Paper 2001-2526, 2001.

[4]Madsen, H., Krenk, S., and Lind, N., *Methods of Structural Safety*, Prentice–Hall, Englewood Cliffs, NJ, 1986, p. 8.

[5]Abumeri, G., Kuguoglu, L., and Chamis, C., "Nondeterministic Optimization: Composite Laminates, Beams, and Blades," AIAA Paper 2000-1565, 2000.

[6]Fowlkes, W., and Creveling, C., *Engineering Methods for Robust Product Design Using Taguchi Methods in Technology and Product Development*, Addison Wesley Longman, Reading, MA, 1995.

[7]Winston, W., *Operations Research—Algorithms and Applications*, 3rd ed., Duxbury, Belmont, CA, 1994, p. 840.

[8]Li, W., Huyse, L., and Padula, S., "Robust Airfoil Optimization to Achieve Drag Reduction over a Range of Mach Numbers," *Structural and Multidisciplinary Optimization* (to be published).

[9]Pratt, J., Raiffa, H., and Schlaifer, R., *Introduction to Statistical Decision Theory*, MIT Press, Cambridge, MA, 1996, pp. 639ff.

[10]Anderson, W., and Bonhaus, D., "An Implicit Upwind Algorithm for Computing Turbulent Flows on Unstructured Grids," *Computers and Fluids*, Vol. 23, No. 1, 1994, pp. 1–21.

[11]Anderson, W., and Bonhaus, D., "Airfoil Design on Unstructured Grids for Turbulent Flows," *AIAA Journal*, Vol. 37, No. 2, 1999, pp. 185–191.

[12]Harris, C. D., "NASA Supercritical Airfoils," NASA TP-2969, 1990.

[13]Marcum, D., "Generation of Unstructured Grids for Viscous Flow Applications," AIAA Paper 95-0212, 1995.

[14]Alexandrov, N., Lewis, R., Gumbert, C., Green, L., and Newman, P., "Approximation and Model Management in Aerodynamic Optimization with Variable-Fidelity Models," *Journal of Aircraft*, Vol. 38, No. 6, 2001, pp. 1093–1101.

[15]Drela, M., "Pros and Cons of Airfoil Optimization," *Frontiers of Computational Fluid Dynamics*, edited by D. Caughey and M. Hafez, World Scientific, 1998, pp. 363–381.

[16]Campbell, R., "Efficient Viscous Design of Realistic Aircraft Configurations," AIAA Paper 98-2539, 1998.

[17]Elliott, J., and Peraire, J., "Constrained, Multipoint Shape Optimization for Complex 3D Configurations," *Aeronautical Journal*, Vol. 102, No. 1017, 1998, pp. 365–376.

[18]Saaty, T. L., *Multicriteria Decision Making—The Analytic Hierarchy Process*, RWS Publ., Pittsburgh, PA, 1992.

[19]Messac, A., "From Dubious Construction of Objective Functions to the Application of Physical Programming," *AIAA Journal*, Vol. 38, No. 1, 2000, pp. 155–163.

[20]Gu, X., Renaud, J., Batill, S., Brach, R., and Budhiraja, A., "Worst Case Propagated Uncertainty of Multidisciplinary Systems in Robust Design Optimization," *Structural and Multidisciplinary Optimization*, Vol. 20, No. 3, 2000, pp. 190–213.

[21]Batill, S., Renaud, J., and Gu, X., "Modeling and Simulation Uncertainty in Multidisciplinary Design Optimization," AIAA Paper 2000-4803, 2000.

[22]Hicks, R. M., and Vanderplaats, G. N., "Application of Numerical Optimization to the Design of Supercritical Airfoils Without Drag-Creep," Society of Automotive Engineers, SAE Paper 770440, 1977.

[23]Vanderplaats, G., *ADS–A FORTRAN Program for Automated Design Synthesis*, Engineering Decision Optimization, Santa Barbara, CA, 1987.

[24]"iSIGHT: Designer's Guide, Version 5.5," Engineous Software, Inc., Morrisville, NC, 2000.

[25]Shevell, R., *Fundamentals of Flight*, Prentice–Hall, Englewood Cliffs, NJ, 1989.

[26]Huyse, L., "Free-Form Airfoil Shape Optimization Under Uncertainty Using Maximum Expected Value and Second-Order Second-Moment Strategies," Inst. for Computer Applications in Science and Engineering, Rept. 2001-18/NASA CR 2001-211020, Hampton, VA, 2001.

E. Livne
Associate Editor